Mg doping of InGaN layers grown by PA-MBE for the fabrication of Schottky barrier photodiodes

J Pereiro, A Redondo-Cubero, S Fernandez-Garrido, C Rivera, A Navarro, E Muñoz, E Calleja, R Gago, Juan Pereiro

Mg doping of InGaN layers grown by PA-MBE for the fabrication of Schottky barrier photodiodes

J.Pereiro[1,*], A. Redondo-Cubero[1,2], S. Fernandez-Garrido[1], C. Rivera[1], A. Navarro[1], E. Muñoz[1], E. Calleja[1] , R. Gago[3].

[1] *Instituto de Sistemas Optoelectrónicos y Microtecnología, Universidad Politécnica de Madrid, E-28040 Madrid, Spain*

[2] *Centro de Micro-Análisis de Materiales, Universidad Autónoma de Madrid, E-28049 Madrid, Spain*

[3] *Instituto de Ciencia de Materiales de Madrid, Consejo Superior de Investigaciones Científicas, E-28049 Madrid, Spain*

ABSTRACT

This work reports on the fabrication of Schottky barrier based Mg-doped (In,Ga)N layers for fluorescence applications. Mg acceptors are used in order to compensate surface and bulk donors that prevent the fabrication of Schottky contacts on unintentionally doped (In,Ga)N layers. Rectifying properties of the contacts exhibited a major improvement when (In,Ga)N:Mg is used. The electrical and optical measurements of the layers showed a hole concentration up to 3×10^{19} holes/cm^3 with a Mg acceptor activation energy of ~60 meV. Backilluminated photodiodes fabricated on 800 nm thick Mg-doped $In_{0.18}Ga_{0.82}N$ layers exhibited a band pass photo-response with a rejection ratio $>10^2$ between 420 nm and 470 nm and peak responsivities of 87 mA/W at ~470 nm. The suitability of these photodiodes for fluorescence measurements was demonstrated.

PACS: 68.35.bg; 85.30.De; 85.60.Gz; 81.15.Hi

[*] Juan Pereiro (jpereiro@die.upm.es). Instituto de Sistemas Optoelectrónicos y Microtecnología, Universidad Politécnica de Madrid, E-28040 Madrid, Spain

INTRODUCTION

Applications such as solar UVA monitoring, biophotonics, hydrocarbon combustion control and fluorescence spectroscopy requires the detection of visible (VIS) light. Si-based photodiodes are the most popular devices in this range of wavelengths. However, (In,Ga)N technology shows important advantages, the bandgap can be tuned from 0.7 eV to 3.4 eV, so a high spectral selectivity can be obtained without using external filters. (In,Ga)N-based devices also allow the monolithic integration of different optical elements in a single structure and they show better behaviour at high temperature, less degradation in harsh environments and, potentially, lower dark currents than narrow bandgap semiconductor based photodiodes [1].

Not much work has been carried out on (In,Ga)N-based photodetectors fabricated from thick layers, since the low miscibility of GaN and InN and the low dissociation energy of the In-N bond give rise to problems such as phase separation, alloy segregation, clustering or decomposition during growth. Moreover, surface and bulk donor concentrations increase with the In content of the alloy, preventing the possibility of obtaining good rectifying contacts on the surface of this ternary [2][3]. Mg doping of (In,Ga)N layers is expected to relieve this problem by introducing acceptors which can compensate residual donors [4]. In device applications, Mg doping of (In,Ga)N layers has also been used to reduce *p*-type ohmic contact resistivity in (In,Ga)N/GaN LEDs, applying a concentration exceeding that required to compensate donors [5]. However, there are not many studies based on the growth by plasma-assisted molecular beam epitaxy (PA-MBE) of Mg doped (In,Ga)N thick layers [4][5][6][7].

In the present work, a study on the Mg doping of (In,Ga)N layers grown by PA-MBE is presented. The electrical, optical and structural properties of the samples were studied allowing a better understanding of the behaviour of the Mg atoms and their effects on (In,Ga)N layers. Acceptor and hole concentrations as well as the activation energy of the Mg impurities were determined. The

possibility of obtaining good rectifying properties on (In,Ga)N layers was checked by fabricating Schottky barrier (SB) photodiodes (PDs) for fluorescence applications.

EXPERIMENTAL

The experiment consisted of studying the behaviour of (In,Ga)N growth using different Mg effusion cell temperatures. The (In,Ga)N:Mg layers were grown by PA-MBE using a Riber Compact 21s system equipped with an Addon rf-plasma N source and Knudsen effusion cells for In, Ga and Mg. Commercial (Lumilog) (0001)-GaN templates grown by metal-organic vapour phase epitaxy (MOVPE) on *c*-plane sapphire with a threading dislocation density in the $1\text{-}10\times10^{8}$ cm^{-3} range were used as substrates. Their backsides were coated with Ti for efficient heat absorption during growth. The substrate temperature was measured using an Ircon Modline 3 optical pyrometer. After a chemical degrease, the substrates were introduced into the MBE system and outgassed during 30 min at 400 °C. Prior to the (In,Ga)N growth, a 100-nm-thick GaN buffer layer was grown at 730 °C under intermediate Ga-rich conditions to obtain a smooth and flat surface [8]. The N_2 partial pressure in the growth chamber was kept at 1.1×10^{-5} Torr during growth.

The composition and the structural quality of the (In,Ga)N compounds were studied by Rutherford backscattering spectrometry (RBS) using a 2 MeV He^{+} ion beam with a 1 mm^2 spot. Channelling measurements (RBS/C) along the <0001> axis of the wurtzite structure were carried out to determine crystal quality with depth resolution. Both random and <0001> aligned spectra were acquired in *IBM* geometry with the detector placed at a scattering angle of 170°. Sample position was controlled by a three-axis goniometer with 0.01° of accuracy. Experimental data were simulated using the *RBX* program [9]. Complementary characterization of the crystal quality and alloy compositions was performed by XRD and absorption measurements using a Jasco V650 spectrophotometer and a triple-axis Bede D^3 diffractometer respectively.

Mg-doping level and hole concentration have been studied by means of C-V and Hall effect measurements. RBS measurements could not be used in this case, because the amount of Mg was

below the detection limits due to the low scattering cross-section of Mg and the Ga background. Since the Mg-fluxes used for doping were below the sensitivity of the Bayard-Alpert, the fluxes are indicated in cell temperature units.

Hall measurements were performed using the Van der Pauw geometry. Ohmic contacts were made of In. The hole concentration, obtained by this method, was compared to the acceptor concentration determined from *C-V* measurements using a Hg profiler. In order to confirm these results, Schottky diodes were fabricated on the (In,Ga)N:Mg layers by depositing Ti (50 nm) /Al (200 nm) Schottky contacts with a circular geometry. Ni (50nm) /Au (200 nm) extended Ohmic contacts were alloyed at 400ºC for 10 minutes in order to reduce its resistance.

GROWTH AND STRUCTURAL CHARACTERIZATION

The structural quality of undoped-(In,Ga)N samples was studied by measuring the minimum yield (χ_{min}) along the whole range of In compositions. The minimum yield (χ_{min}) is defined as the ratio between the aligned and the random yield, that was determined from RBS/C spectra along <0001> for In atoms. This parameter quantifies the crystalline quality of the sample and its value is related with the percentage of disordered atoms inside the layer. The energy scale is also related to the depth of the layer and, therefore, χ_{min} can be analyzed at different regions. Results indicate that χ_{min} gradually increases, reaching a maximum of ~25% for intermediate In contents ($0.4<x<0.8$). This result is a clear evidence of the loss of crystal quality, mostly associated to miscibility problems. For low and high values of *x*, the minimum yield values are comparable with that of the GaN template used as substrate (2-5%), and only a remaining dechannelling is visible in the spectra [10]. Since the structural quality of (In,Ga)N layers with In contents around 0.5 was found to be poor, an In content around 0.2-0.3 was the best choice in order to perform the doping studies. Reflection-high-energy-electron diffraction (RHEED) observations during growth showed a streaky pattern and 2D growth was obtained for samples $x<0.30$. Finally, an In content of $x\approx0.2$ was chosen as a compromise of sample quality, reproducibility and usefulness. The expected bandgap wavelength matches with the

emission of some common fluorophores, *i.e. Pacific Blue* (~460 nm), which is usually utilized for the detection of proteins and nucleic acids. This may allow us to fabricate fluorescence sensors where the emitter, the optical filter and the photodetector are all based on III-N compounds.

The same growth conditions including, III-element fluxes, temperature, N_2 pressure, and N flux, were utilized for all the samples. The fluxes were calibrated in potential (0001)-(In,Al,Ga)N growth units (nm/min) [11]. N flux of ~8 nm/min, and Ga and In fluxes of ~5 nm/min and ~1.5 nm/min were used, respectively. No In droplets were observed on the samples at the end of the growth. A summary of the samples used for the different measurements can be found in Table 1. The substrate temperature was fixed at 600ºC for all cases. The only parameter that was varied was the Mg cell temperature. Four samples of 200 nm of $In_{0.18}Ga_{0.82}N$:Mg were grown in order to measure RBS. The Mg cell temperatures used for this study were 235 ºC, 240 ºC, 245 ºC and 250 ºC. Thicker samples parallel carrier conduction through the GaN-(In,Ga)N interface [12]. Seven $In_{0.18}Ga_{0.82}N$:Mg layers with a nominal thickness of 800 nm were grown. Mg temperatures between 225 ºC and 275 ºC were used in this case.

RHEED pattern was streaky during the growth of low doped (In,Ga)N layers, what is a characteristic from 2D growth mode. However, the increase in Mg flux leads to a brighter pattern up to 250 ºC. Over this temperature the RHEED started to show a slightly spotty pattern, and at a Mg cell temperature of 275 ºC, it became completely spotty. These changes in the RHEED pattern point out that above 250 ºC a degradation of the InGaN surface morphology occurs. A 1×3 RHEED reconstruction was observed at the end of the growth of each layer, indicating that all the In on the surface, except a third of a monolayer, was consumed while the substrate temperature was decreased, once the shutters were closed [13][14]. The reconstruction was also observed in the undoped samples. The only exception is the sample with the higher Mg flux, which did not show any reconstruction due to its poor structural quality.

RBS measurements of the Mg-doped $In_{0.18}Ga_{0.82}N$ samples reveal a constant and homogeneous concentration of In, Ga and N in the samples, with no interface effects. Figure 1 shows the RBS <0001> channelled and random spectra for the InGaN:Mg sample with a hole concentration ~3×10^{19} cm^{-3}. Channelling experiments showed a similar minimum yield (χ_{min}~18%) for all the samples independently of the Mg concentration. Important variations were not observed in χ_{min} for samples grown with Mg cell temperatures below 250 ºC. However, the measured minimum yield value is slightly higher than the one obtained for non-intentionally doped $In_{0.18}Ga_{0.82}N$ layers (χ_{min}=12.5%), indicating the interstitial incorporation of Mg atoms. The amount of interstitial Mg atoms seems to remain constant up to a Mg flux corresponding to a cell temperature of 250ºC.

The intensity of XRD $In_{0.18}Ga_{0.82}N$ diffraction maxima decreased and the peaks became broader as the Mg flux was higher (Fig 2**Error! Reference source not found.**a). An increase of the absorption edge width confirmed XRD results (Fig. 2b). Both measurements indicate a degradation of the samples when Mg cell temperature above 250 ºC was used. Further XRD experiments were performed in order to gather more information about the effect of Mg impurities in the InGaN layer. The FWHM of the rocking curves of the layers are shown in Table 1. The behaviour of the FWHM as a function of the Mg flux shows a similar trend to the one expected for GaN:Mg. The FWHM is lower than the one for the undoped samples when low Mg fluxes were used, indicating the surfactant effect of Mg during growth. As the Mg flux is increased the structural quality of the layer deteriorates and a higher FWHM is found. The evolution suggests that a higher Mg flux induces the appearance of a higher number of misorientations in the crystal, which may be due, as in GaN:Mg, to the generation of N-polar inclusions. The apparent disagreement between χ_{min} and the FWHM of the rocking curves as a function of the Mg flux is explained due to the different sensitivity of both measurements: χ_{min} is much more sensitive to interstitial defects, while XRD is more sensitive to misorientations in the crystal.

ELECTRICAL CHARACTERIZATION

As stated above Schottky photodiodes fabricated on InGaN show very poor rectifying properties. The effect of the Mg doping of the material on the IV curves of the devices is shown in Fig 3, there is a clear reduction of the current and an improvement of the rectifying behaviour of the devices (it is important to keep in mind that Mg doped InGaN is a p-type material so the forward bias happens when negative voltages are applied to the Schottky contact).

Electrical characterization measurements are summarized in Fig. 4. The trend of the hole and acceptor concentrations is clear; despite that at low carrier concentrations Hall measurements could not be performed due to the poor quality of ohmic contacts. As the carrier concentration increases, the Ohmic contacts improve, but worse rectifying properties are obtained for Schottky contacts and no meaningful *C-V* measurements are achieved for the sample with the highest hole concentration. These are the reasons for the missing points in Fig. 4, the C-V measurements for the lowest Mg fluxes and the Hall measurement for the highest Mg flux.

A maximum hole concentration of 3×10^{19} cm^{-3} is reached at a Mg cell temperature of 250 ºC with a mobility value at room temperature of 4 cm^2/Vs, comparable to the ones obtained by MOVPE growth [15]. Therefore, it is shown that it is possible to obtain similar, and even higher, concentrations to those obtained by metal-organic vapour phase epitaxy [15]. All the results obtained suggest that Mg doping of (In,Ga)N and GaN are similar. In both cases a maximum hole concentration is reached at a certain Mg flux. If a higher Mg flux is used, hole concentration decreases and a degradation of the structural properties of the layer occurs, this effect is what I will be calling overdoping. In GaN, an excess of Mg causes a layer polarity inversion, inducing material degradation and decreasing the efficiency of substitutional incorporation of Mg atoms [13][16][17]. Taking into account our results, the same processes are expected. In our case, 250 ºC corresponds to the higher Mg flux that can be used in order to obtain an efficient incorporation of Mg atoms in $In_{0.18}Ga_{0.82}N$ substitutional positions.

The activation energy can be determined from the difference between the acceptor concentration values extracted from *C-V* measurements and the deduced hole concentration values from Hall measurements. However, in order to improve the accuracy of the resulting activation energy values of the Mg acceptors, Hall effect measurements as a function of temperature were performed.

Samples with intermediate hole concentrations were evaluated by Hall measurements as a function of temperature, as shown in Fig. 5. The data has been fitted using the charge neutrality condition described in [18] as

$$p(T) = \frac{N_a}{1 + \frac{p(T)g}{N_V}\exp\left(\frac{\Delta E_a}{k_B T}\right)} - N_D, \qquad (1)$$

where N_V is the valence band density of states, ΔE_a is the activation energy of the acceptors, $p(T)$ is the hole concentration, N_a is the acceptor concentration, N_D is the donor concentration, k_B is the Boltzmann constant and T is the temperature. An acceptor degeneracy factor g = 2 was used [19]. The activation energy obtained with eq. (1) in the $In_{0.18}Ga_{0.82}N$ layers is ~60±5meV. Although, no data has been found in the literature for Mg doped (In,Ga)N samples grown by MBE, our results are in agreement by extrapolating the data presented by Kumakura *et al.* for $In_xGa_{1-x}N$:Mg with $x \leq 0.14$ [15] grown by MOVPE. PL results (not shown) seem to support the results presented above.

PHOTODETECTOR CHARACTERIZATION

As expected, current-voltage (*I-V*) characteristics of the Schottky barrier diodes (not shown) show a current increase as the *p*-type doping of the layer increases. Once a Mg cell temperature of 250 ºC is exceeded, the current decreases, at the same time that the hole concentration does. However, rectifying characteristics of the contacts improve in comparison to the ones fabricated on unintentionally-doped (In,Ga)N samples.

The (In,Ga)N:Mg photodiodes were used in a back-illuminated configuration, in order to use GaN substrate as an optical filter. The spectral response is plotted in Fig. 6. The peak responsivity is as high as 90 mA/W at 470 nm, and there is a contrast of $>10^2$ between 420 and 470 nm.

The self-filtering effect from the InGaN layer occurs since the thickness of the $In_{0.18}Ga_{0.82}N$ layers is larger than the diffusion length of the carriers. The carriers photogenerated far from the depletion region of the diode, at a longer distance than the diffusion length, do not contribute to the photocurrent. The inset of Fig. 6 shows the spectral response of the diodes in a logarithmic scale. Here, it is possible to observe how as Mg doping of the layer grows, optical filtering increases and less photocurrent at higher energies is obtained, due to a decrease of diffusion length of photogenerated carriers.

In order to explain the changes in the peak responsivity wavelength between the samples, a simple model based on the absorption of the samples has been developed. A diffusion length of 150-200 nm is assumed for the heavier doped sample as a starting point. This value is the estimated minority carrier diffusion length in *p*-type GaN [20]. Although the diffusion length for (In,Ga)N is expected to be higher [21][22], the heavy doping of the sample should reduce it, so the value for GaN is adequate. The model is described in the inset of Fig 7, different regions of the same InGaN layer act as an optical filter and as active layer. The calculations consist of the subtraction of the absorption that occurs in the non-active region of the InGaN layer from total absorption. We assume that the thickness of the active region of the heaviest doped diode is 200 nm, and that it varies as a function of the acceptor concentration as the experimental thickness of the SCR does. The total absorption of the layers is taken from experimental measurements.

The normalized spectral response given by this model is shown in Fig 7. The relative positions of the peak responsivities as a function of the Mg doping are very similar to that experimentally obtained. This seems to indicate that the changes in the maximum responsivity wavelength of the diodes are due to small changes in the In content or the strain of the layers. The small differences

observed between the maxima peak wavelengths of the experimental results and the theoretical results are attributed to differences between the actual diffusion length and the one considered in the calculations. The different behaviour of the layer growth with a Mg cell temperature above 250 ºC seems to be related to the structural problems of this layer, which, in turn, could affect carrier diffusion length.

The main application for this photodiodes is fluorescence measurements, and the integration of the detector and the optical filter in one structure. Fig. 8 shows the superposition of the spectral response of one of the $In_{0.18}Ga_{0.82}N$:Mg SB PDs and the excitation-emission spectra of the *Pacific Blue* dye, which is a commercial fluorophore used to label proteins and nucleic acids [23][24]. It is shown how the back-illuminated $In_{0.18}Ga_{0.82}N$:Mg Schottky barrier photodiodes are able to filter the excitation emission of common dyes used in this kind of experiments. It is concluded that this photodiodes are suitable for fluorescence experiments.

CONCLUSIONS

In this work, a detailed study on the Mg doping of InGaN has been carried out. Mg doping of InGaN layers as a function of Mg flux behaves similarly to Mg doping of GaN. A maximum carrier concentration of $3\times10^{19}cm^{-3}$ was obtained for a certain Mg flux, and if this Mg flux is exceeded, the carrier concentration decreases and a deterioration of the structural quality of the sample occurs. The activation energy of the Mg acceptors in $In_{0.18}Ga_{0.82}N$ measured by PL and Hall measurements as a function of temperature is ~60±5 meV, in good agreement with the values extracted from MOVPE experiments carried out on $In_xGa_{1-x}N$ with $x \leq 0.14$.

Mg doping of InGaN layers allows to overcome problems regarding to high donor residual concentrations, and to the increase of donor surface states as a function of In content. Good rectifying contacts have been obtained on InGaN. A band pass spectral response is observed for backilluminated (In,Ga)N:Mg based Schottky barrier (SB) photodiodes. The optical filtering

increases with hole concentration. The suitability of the SB PDs for fluorescence measurements is demonstrated.

ACKNOWLEDGEMENT

This work was partially supported by the CM P-AMB-000374 505 FUTURSEN. Authors also thank financial support by EU-FP6 (MOU 04/102.052/032) and the Spanish MEC (FIS2009-12964-C05-04).

REFERENCES

[1] Muñoz E, 2007, (Al,In,Ga)N-based photodetectors. Some materials issues. *Phys. Stat. Sol. – Basic solid state physics* **244** 2859-2877.

[2] Pereiro J, Pau JL, Rivera C, Navarro A, Muñoz E, Czernecki R, Targowski G, Prystawko P, Krysko M, Leszczynski M and Suski T 2007 InGaN growth applied to the fabrication of photodetector devices *Nitrides and Dilute Nitrides: Growth, Physics and Devices* ed: J. Miguel (Kerala; Transworld Research Signpost).

[3] Bailey LR, Veal TD, King PDC, McConville CF, Pereiro J, Grandal J, Sánchez-García MA, Muñoz E and Calleja E 2008 Band bending at the surfaces of In-rich InGaN alloys *J. Appl. Phys.* **104** 113716.

[4] King PDC, Veal TD, Hai Lu, Jefferson PH, Hatfield SA, Schaff WJ and McConville CF 2008 Surface electronic properties of n- and p-type InGaN alloys *Phys. Stat. Sol. (b)* **245** 881.

[5] Kumakura K, Makimoto T and Kobayashi N 2003 Mg-acceptor activation mechanism and transport characteristics in p-type InGaN grown by metalorganic vapor phase epitaxy *J. Appl. Phys.* **93** 3370-3375.

[6] Chen X, Matthews KD, Hao D, Schaff WJ and Eastman LF, 2008 “Growth, fabrication and characterization of (In,Ga)N solar cells”, *Phys. Stat. Sol. (a)* **205** 1103–1105.

[7] Berkman EA, El-Masry NA, Emara A and Bedair SM 2008 Nearly lattice-matched n, i, and p layers for (In,Ga)N p-i-n photodiodes in the 365–500 nm spectral range *Appl. Phys. Lett.* **92** 101118.

[8] Koblmüller G, Fernandez-Garrido S, Calleja E and Speck JS 2007 In situ investigation of growth modes during plasma-assisted molecular beam epitaxy of (0001) GaN *Appl. Phys. Lett.* **91** 161904.

[9] Kótai E 1994 Computer methods for analysis and simulation of RBS and ERDA spectra *Nucl. Instrum. Methods Phys. Res., Sect. B* **85** 588.

[10] Redondo-Cubero A, Pereiro J, Grandal J, Lorenz K, Franco N, Gago R, Muñoz E, Sánchez-García MA, Calleja E and Alves E, 2009 Structural study of the epitaxial growth in InGaN/GaN heterostructures by ion beam analysis *WOCSDICE* Málaga (Spain).

[11] Heying B, Averbeck R, Chen LF, Haus E, Riechert H and Speck JS 2000 Control of GaN surface morphologies using plasma-assisted molecular beam epitaxy *J. Appl. Phys.* **88** 1855-1860.

[12] P. Blood and J. W. Orton, The Electrical Characterization of Semiconductors: Majority Carriers and Electron States. Academic Press (1992).

[13] Green DS, Haus E, Wu F, Chen L, Mishra UK and Speck JS 2003 Polarity control during molecular beam epitaxy growth of Mg-doped GaN *J. Vac. Sci. Technol. B* **21** 1804.

[1412] Chen H, Feenstra RM, Northrup JE, Zywietz T, Neugebauer J and Greve DW 2000 Surface structures and growth kinetics of (In,Ga)N (0001) grown by molecular beam epitaxy *J. Vac. Sci. Technol. B* **18** 2284-2289.

[15] Kumakura K, Makimoto T and Kobayashi N 2000 Activation energy and electrical activity of Mg in Mg doped $In_xGa_{1-x}N$ ($x<0.2$) *Jpn. J. Appl. Phys.* **39**, L337-L339.

[16] Smorchkova IP, Haus E, Heying B, Kozodoy P, Fini P, Ibbetson JP, Keller S, DenBaars SP, Speck JS and Mishra UK 2000 Mg doping of GaN layers grown by plasma-assisted molecular-beam epitaxy *Appl. Phys. Lett.* **76** 718.

[17] Romano LT, Northrup JE, Ptak AJ and Myers TH 2000 Faceted inversion domain boundary in GaN films doped with Mg *Appl. Phys. Lett.* **77** 2479.

[18] Götz W, Kern RS, Chen CH, Liu H, Steirgerwald DA and Fletcher RM 1999 Hall-effect characterization of III–V nitride semiconductors for high efficiency light emitting diodes *Mat. Sci. Eng.* **B59** 211-217.

[19] Tanaka T, Watanabe A, Amano H, Kobayashi Y, Akasaki I, Yamazaki S, and Koike M 1994 p-type conduction in Mg-doped GaN and $Al_{0.08}Ga_{0.92}N$ grown by metalorganic vapor phase epitaxy," *Appl. Phys. Lett.* **65** 593.

[20] Bandic ZZ, Bridger PM, Piquette EC and McGill TC 1998 Minority carrier diffusion length and lifetime in GaN *Appl. Phys. Lett.* **73** 3276-3278.

[21] Duboz JY, Binet F, Dolfi D, Laurent N, Scholz F, Off J, Sohmer A, Briot O and Gil B 1997 Diffusion length of photoexcited carriers in GaN *Mat. Sci. Eng.* **B50** 289-295.

[22] Rumyantsev SL, Shur MS and Levinshtein ME 2004 Material properties of nitrides. Summary *GaN-based Materials and Devices: Growth, Fabrication, Characterization and Performance* ed: Shur MS and Davis RF (Singapore; World Scientific) pp 1-20.

[23] Wei-Chuan Sun, Gee KR, Haugland RP 1998 Synthesis of Novel Fluorinated Coumarins: Excellent UV-Light Excitable Fluorescent Dyes *Bioorganic & Medicinal Chemistry Let.* **8** 3107-3110.

[24] Telford W, Kapoor V, Jackson J, Burgess W, Buller G, Hawley T and Hawley R 2006 Violet Laser Diodes in Flow Cytometry: An Update *Cytometry Part A* **69A** 1153–1160.

Figure captions

Table 1. Summary of the $In_{0.18}Ga_{0.82}N$ samples used in this study. The layer parameters indicated in the table are the Mg cell temperature used during growth, the Mg concentration of the layer, the minimum yield, full width at half maximum (FWHM) of the rocking curves and the thickness of the layer.

Fig. 1. Random and aligned <0001> RBS spectra of sample R394 (~3×10^{19} hole/cm^3).

Fig. 2. Fig. 2a. Transmission spectra of samples with different Mg fluxes. The Mg cell temperature is also indicated for each case. Fig. 2b. XRD spectra of three representative samples of the Mg doping optimization experiment of $In_{0.18}Ga_{0.82}N$. The Mg cell temperature is indicated for each case.

Fig. 3. Effect of Mg doping of InGaN on the IV curves of the devices. The current-voltage characteristics of an nonintentionally doped sample and of sample R387 (~5×10^{15} hole/cm^3) are shown.

Fig. 4. Summary of the current-voltage and Hall measurements of the set of samples of $In_{0.18}Ga_{0.82}N$. No good Ohmic contacts were achieved for the lightly doped samples and no Schottky contacts were accomplished for the sample with the higher carrier concentration.

Fig. 5. Hall measurements as a function of temperature. Van der Pauw geometry was used. The activation energy of the acceptors in $In_{0.18}Ga_{0.82}N$ was fitted to be 60 meV.

Fig 6. Spectral response of the SB PDs fabricated on $In_{0.18}Ga_{0.82}N$:Mg. The Inset show the same curves in a logarithmic scale.

Fig 7. Normalized theoretical spectral response of the photodiodes. The inset shows the structure used for modelling.

Fig 8. Superposition of the spectral response of one of the $In_{0.18}Ga_{0.82}N$:Mg SB PDs and the excitation and emission spectra of the Pacific Blue dye.

Sample	Mg cell temperature (ºC)	Hole concentration (cm^{-3})	χ_{min}	FWHM(º) (Rocking curve)	Thickness (nm)
R387	225	~5×10^{15}	-	-	~800
R391	235	~1×10^{17}	-	0.25	~800
R400	240	9×10^{17}	-	0.35	~800
R401	245	4×10^{18}	-	0.40	~800
R386	250	3×10^{19}	-	0.42	~800
R390	260	2×10^{18}	-	0.43	~800
R385	275	2×10^{18}	-	0.43	~800
R393	236	9×10^{16}	18.5	-	163
R398	240	~8×10^{17}	18.2	-	159
R399	245	~4×10^{18}	16.7	-	161
R394	250	~3×10^{19}	18.1	-	160
R355	-	-	12.5	0.34	300

Table 1. Summary of the InGaN samples used in this study. Hole concentration was calculated directly from hole measurements or approximated from the results obtained by CV measurements.

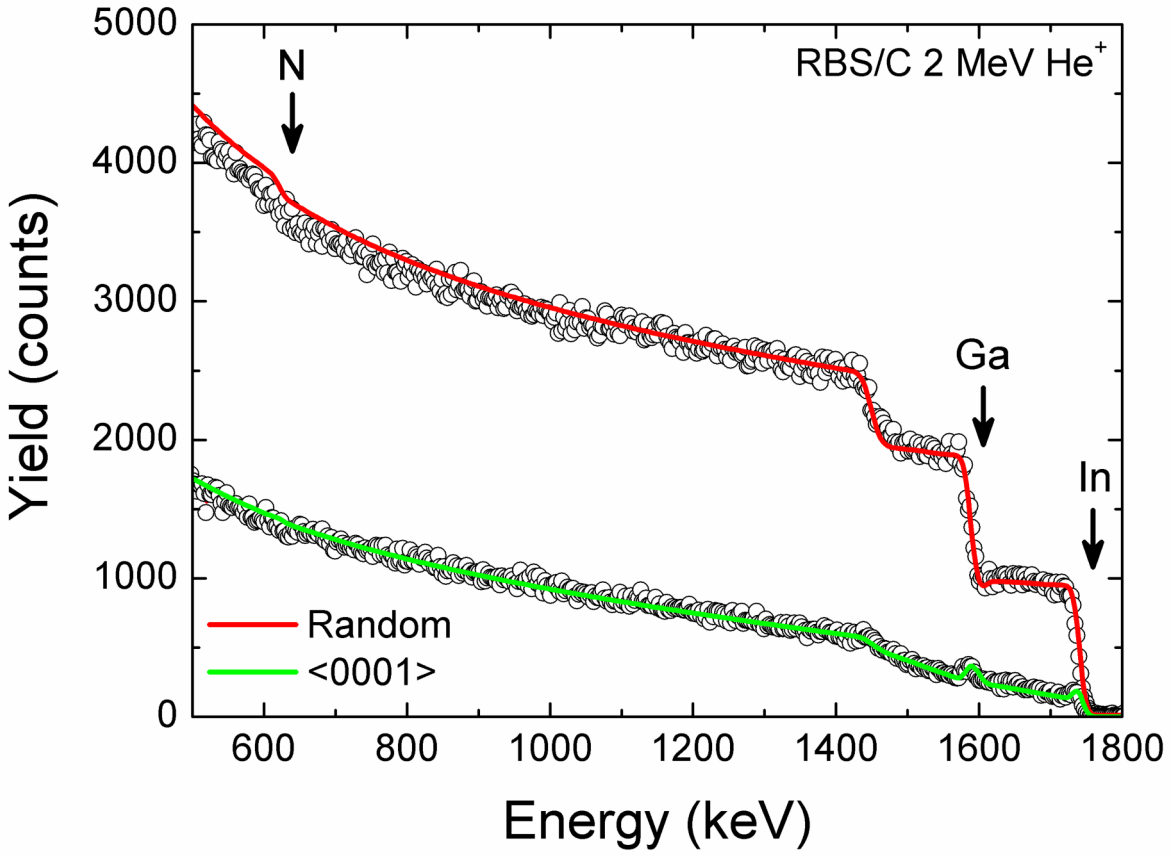

Figure 1 (figure1.TIF)

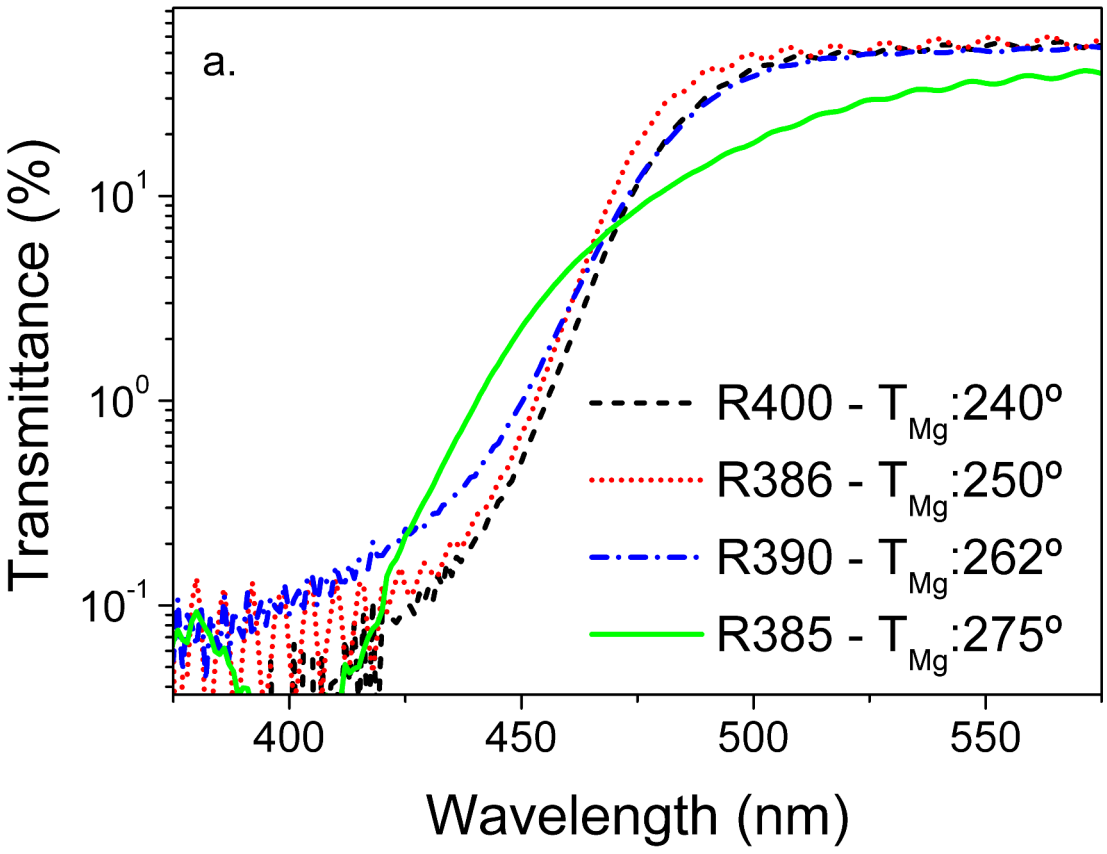

Figure 2a (figure2a.tif)

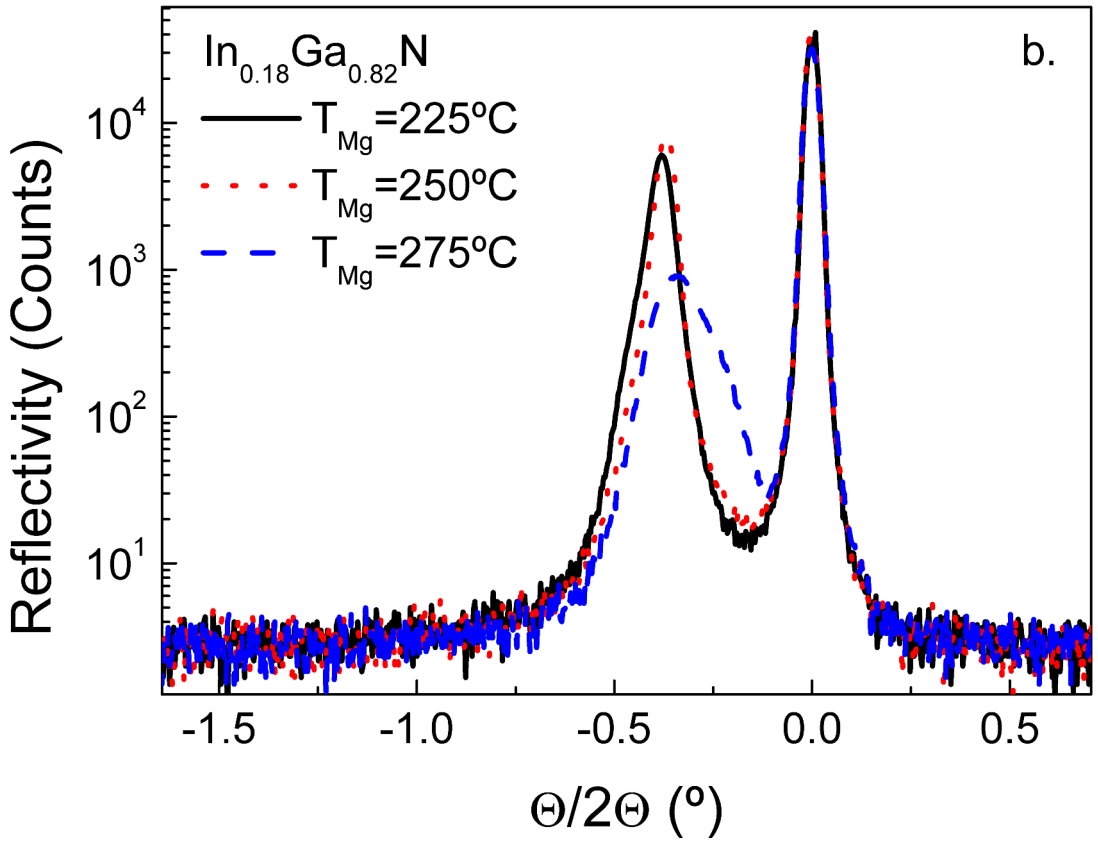

Figure 2b (figure2b.tif)

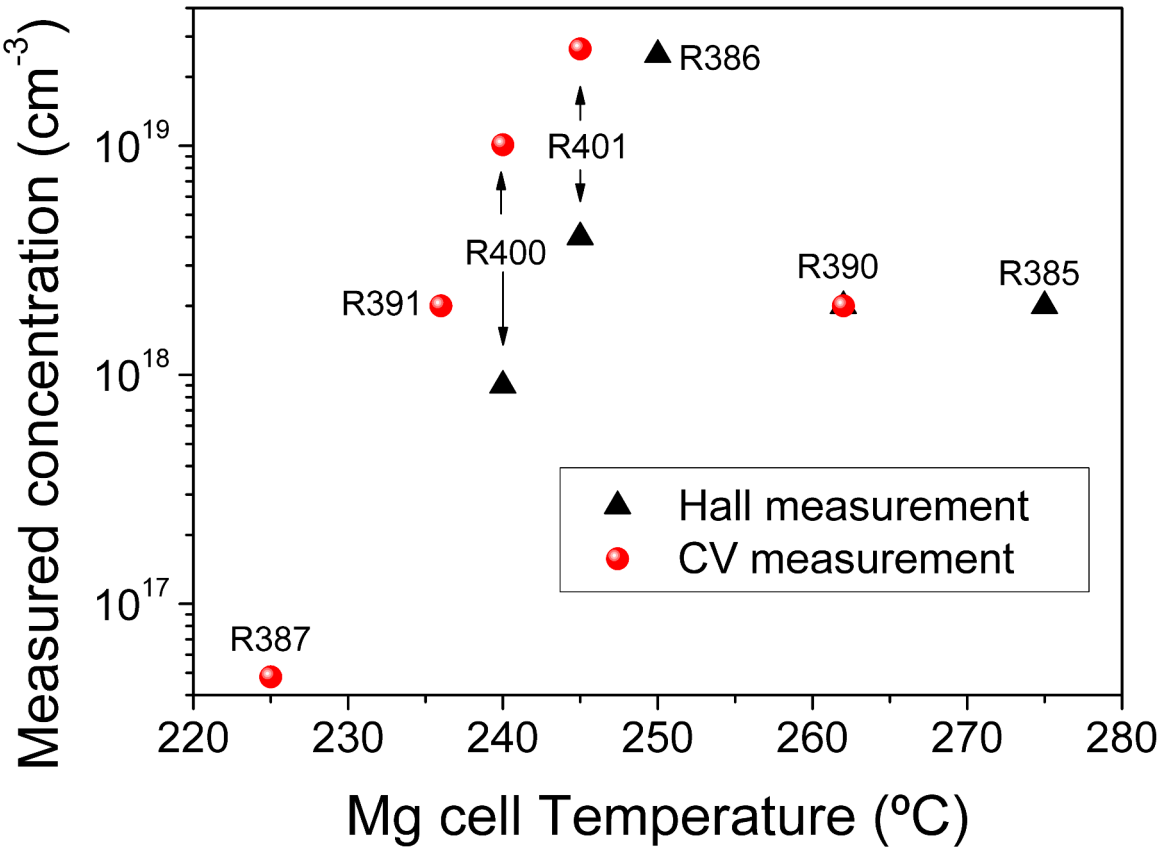

Figure 3 (figure3.tif)

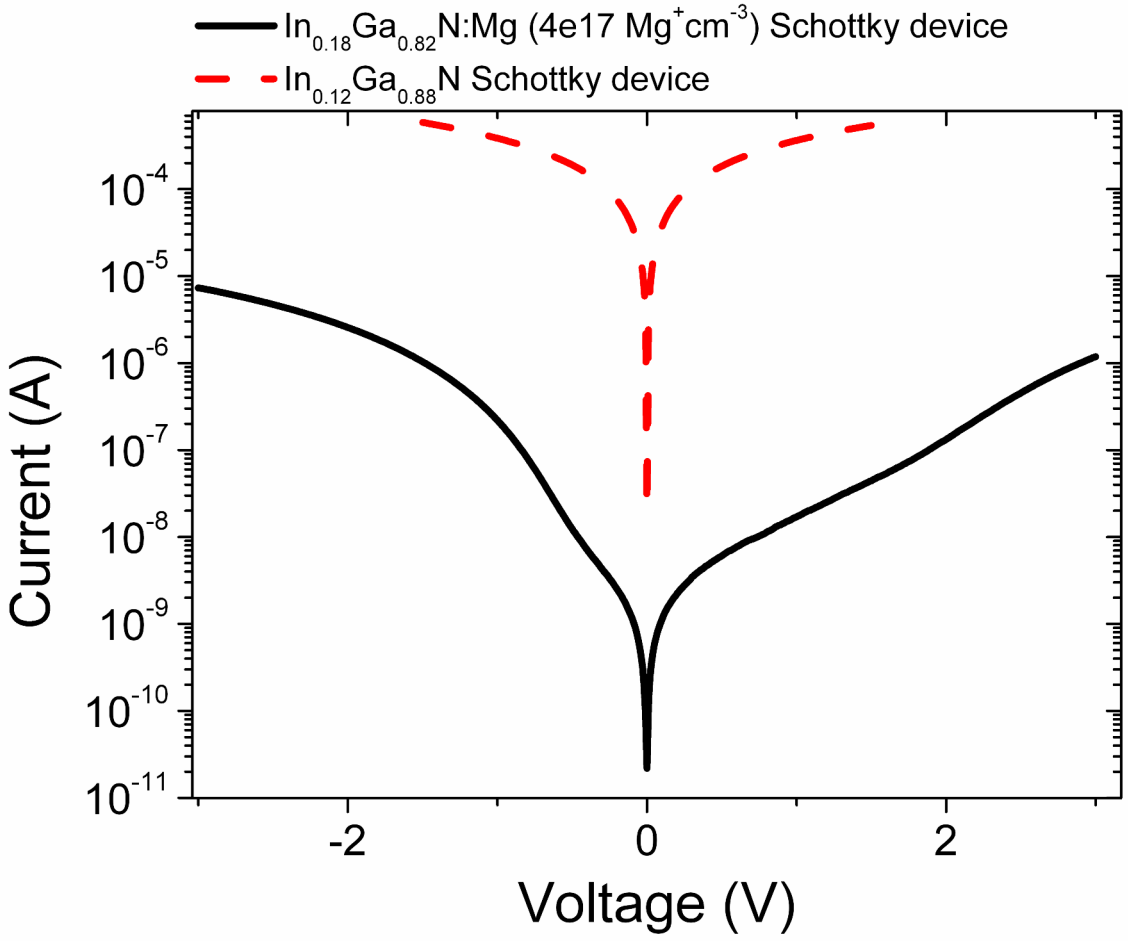

Figure 4 (figure4.TIF)

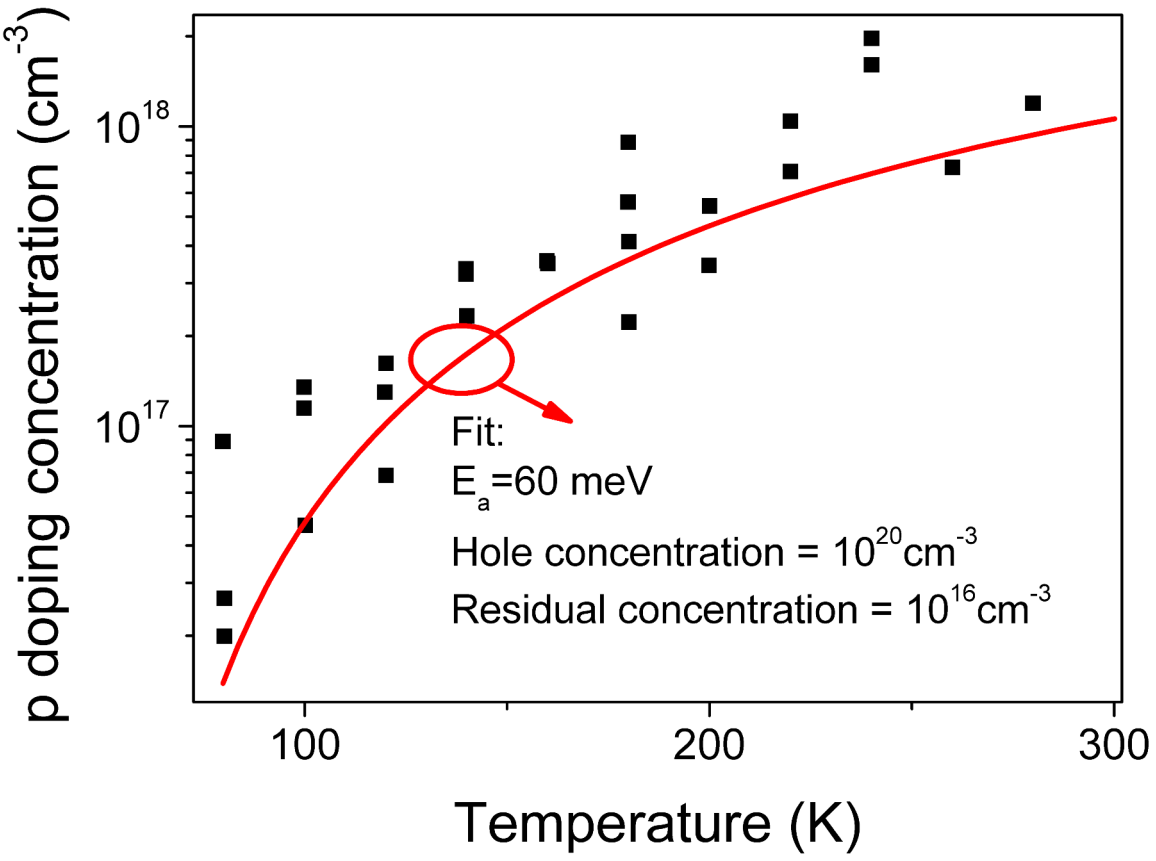

Figure 5 (figure5.tif)

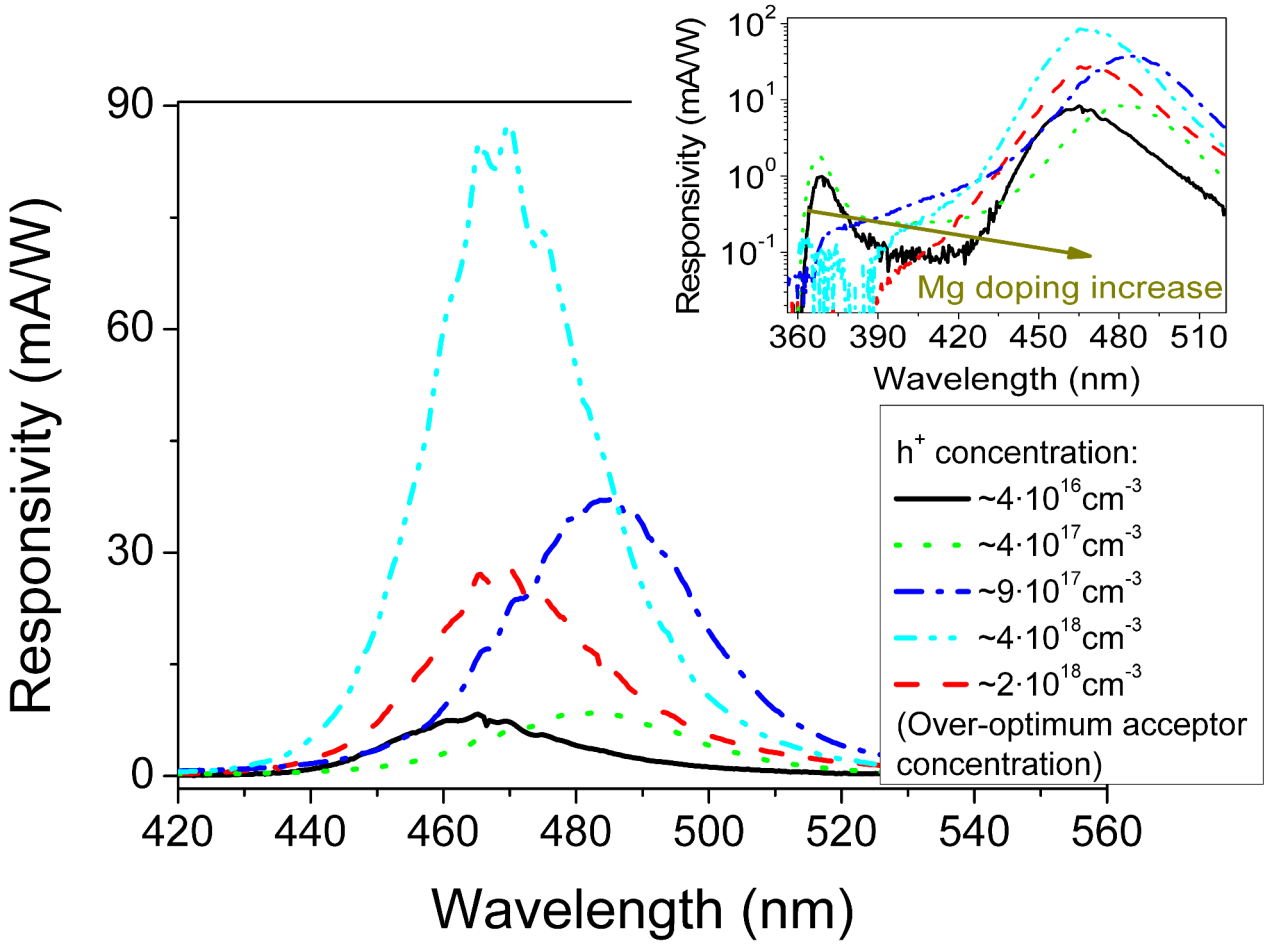

Figure 6 (figure6.tif)

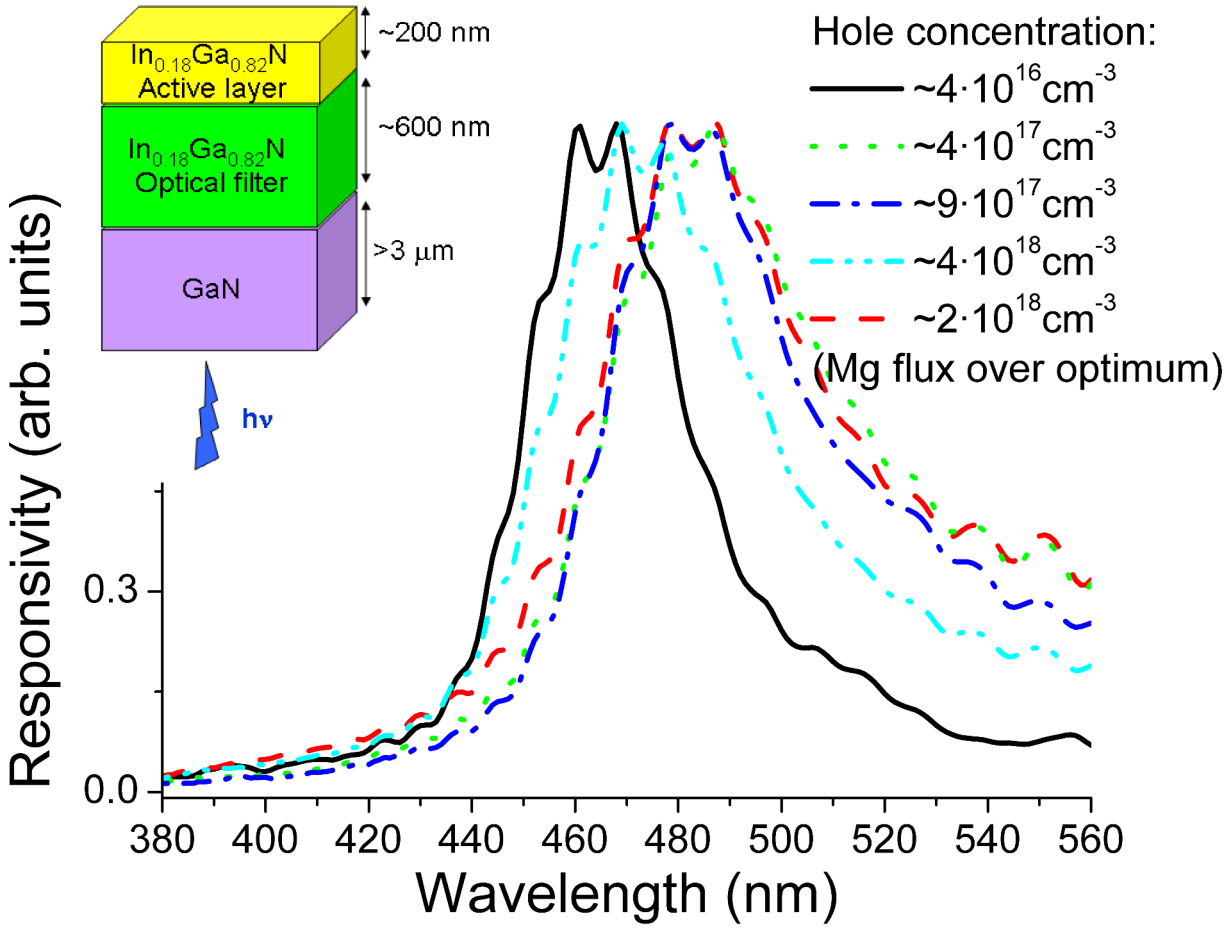

Figure 7 (figure7.tif)

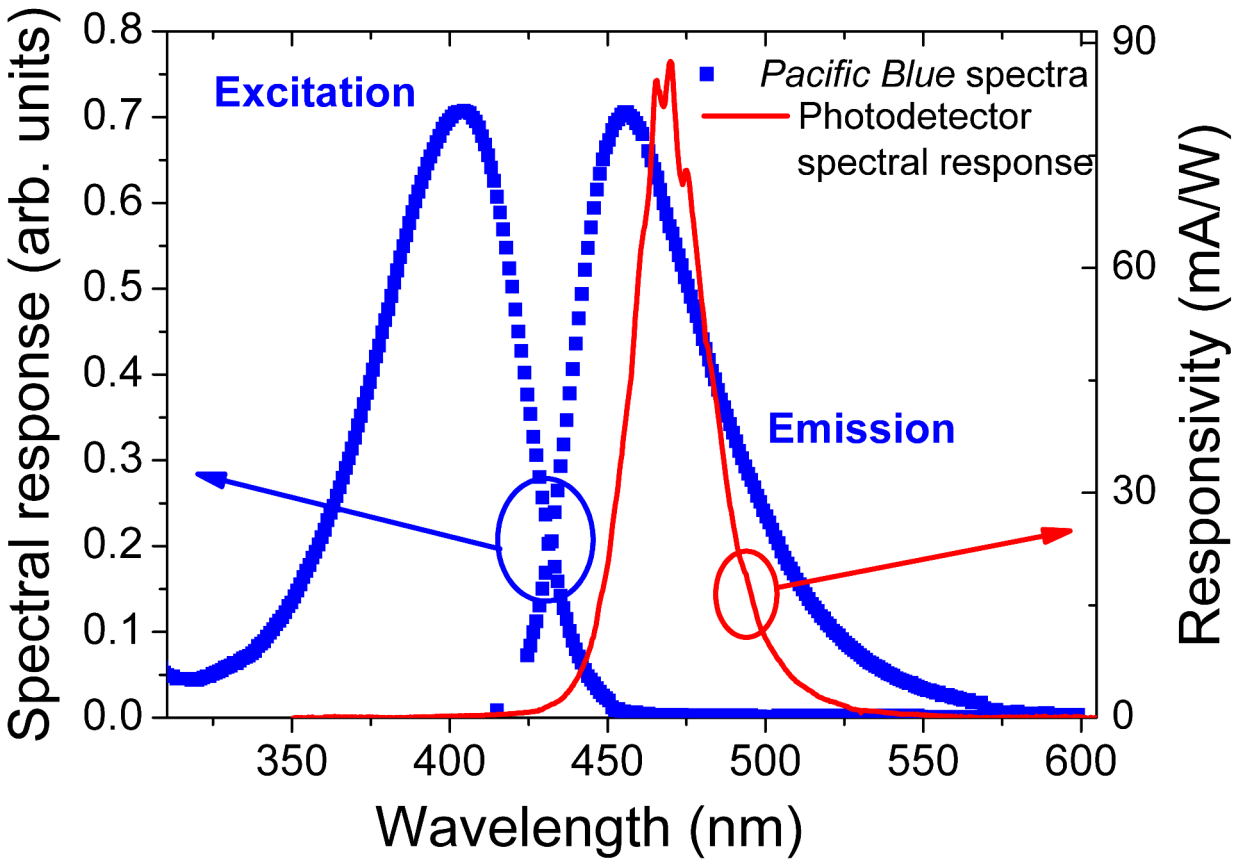

Figure 8 (figure8.tif)